Research paper

Effect of molar ratio on mechanical properties and water resistance of citric acid modified magnesium sulfate cement

Qiaoli Zhang[1], Kun Fan[2]

Abstract: Magnesium oxysulfate (MOS) cement is an ecological inorganic cement-based material. It has several excellent properties, such as high-volume stability, light weight, low thermal conductivity, and high temperature resistance. In this study, the influences of $MgO : MgSO_4 : H_2O$ molar ratio on the mechanical properties and water resistance of modified MOS cement incorporating citric acid were investigated, and the change of pore structure and phase compositions were analyzed by mercury intrusion porosimetry (MIP), X-ray diffraction (XRD) and thermogravimetric (TG) analysis. The results show that when $n(MgO) : n(MgSO_4)$ or $n(MgSO_4) : n(H_2O)$ is larger, the compressive strength and flexural strength of MOS cement paste increase. With the increase of MgO mole number, the softening coefficient of compressive strength decreases, while the softening coefficient and volume shrinkage of flexural strength increase. The total porosity and the most probable aperture of paste with $n(MgO) : n(MgSO_4) : n(H_2O) = 8 : 1 : 20$ are the largest, and smaller molar number of MgO or larger the mole number of H_2O correspond to higher pore structure parameters of cement paste. In addition, with the increase of $n(MgO)/n(MgSO_4)$, the peak intensity of 517 phase is higher, while that of $Mg(OH)_2$ is relatively weak. The content of 517 phase in MOS cement paste with the molar ratio of $10 : 1 : 16$ reaches the maximum.

Keywords: magnesium oxysulfate cement, molar ratio, mechanical properties, water resistance, microstructural analysis

---

[1]MEng., Henan Open University, Zhengzhou 450046, Henan, China, e-mail: zhangqiaoli202@126.com, ORCID: 0009-0001-7975-9903
[2]MEng., Henan Open University, Zhengzhou 450046, Henan, China, e-mail: fk101fk@outlook.com, ORCID: 0009-0009-8237-4703

1. Introduction

Portland cement (PC) is one of the most widely used cement products in the field of building materials. It has the characteristics of fast setting and hardening, high early and late strength and good durability [1,2]. Traditional PC has made great contribution to the progress of human society and economic development, but also gradually exposed some problems. The production process of PC will consume a lot of energy and emit huge amounts of carbon dioxide and fine dust, which will affect and destroy the living environment of human beings [3–5]. Therefore, it is necessary to find a more sustainable cement for construction.

Cement can be divided into calcium cement and magnesia cement according to the main constituent element of cement clinker or its hydration products. The primary representative of calcium cement is PC, while magnesium cement mainly includes magnesium oxysulfate (MOS) cement [6], Magnesium oxychloride (MOC) cement [7] and magnesium phosphate cement (MPC) [8]. MOS cement is a kind of energy-saving material with excellent performance. It can be used as refractory, plastic reinforcement and commercial production of lightweight insulating boards/panels [9–11]. Compared with magnesium oxychloride cement, MOS cement has little corrosion effects to steel bars [12]. The main raw materials of MOS cement are light-burned magnesia and magnesium sulfate heptahydrate [13,14]. Light-burned magnesia is mainly calcined from magnesite at $700 \sim 900°$, while the calcination temperature of PC clinker needs to reach $1450°$. In contrast, the energy consumption of light-burned magnesia is much lower [15,16]. Moreover, magnesium sulfate heptahydrate, one of the main raw materials of MOS cement, can be made from industrial waste [17]. MOS cement is the development direction of magnesium cementitious materials in the future.

MOS cement is a kind of gas hardening cementitious material composed of $MgSO_4$, MgO and H_2O in a certain proportion. The main component of MOS cement after sufficient hydration is $xMg(OH)_2 \cdot yMgSO_4 \cdot zH_2O$ [18,19]. Many researchers have studied the phase composition of MOS cement. Demediuk et al. [20] analyzed the magnesium sulfate cement samples prepared at $30 \sim 120°$ by X-ray diffraction, and he found that there were three crystal phases in hardened paste at $30°$: $Mg(OH)_2$, $3Mg(OH)_2 \cdot MgSO_4 \cdot 8H_2O$ (318 phase) and $MgSO_4 \cdot 7H_2O$. When the temperature is higher, $5Mg(OH)_2 \cdot MgSO_4 \cdot 3H_2O$ (513 phase), $Mg(OH)_2 \cdot MgSO_4 \cdot 5H_2O$ (115 phase) and $Mg(OH)_2 \cdot MgSO_4 \cdot 3H_2O$ (123 phase) were formed. Urwongse and Sorrell [21] applied the chemical equilibrium phase diagram to $MgO–MgSO_4–H_2O$ ternary system, and results showed that in addition to 318 phase, there were 115 metastable phases and $Mg(OH)_2$ in the hydration products at room temperature. Furthermore, a large number of unreacted $MgSO_4 \cdot nH_2O$ (n = 7, 6, 4, 1) and MgO were also found. It is also considered that MgO and $MgSO_4$ solution cannot be used to produce MOS cement with more than 50 wt.% 318 phase at $23°$. These results reveal the reason for the low mechanical strength of MOS cement from the perspective of hydration products.

The hydration system of MOS cement is alkaline, and the alkalinity will gradually increase with the precipitation of basic magnesium sulfate or basic magnesium chloride crystal, and release a lot of heat. In the absence of any chemical modifier, $Mg(OH)_2$ crystals with loose structure are easily formed due to the strong alkalinity of the system, which is the incomplete hydration products of magnesium oxide [13,22]. Meanwhile, the hydration rate cement is too

fast and a lot of heat is released in a short time, resulting in the volume expansion of MOS paste. Therefore, it is usually necessary to add acid modifier to improve the mechanical properties of MOS cement. Some researches suggest that citric acid can significantly improve the strength of hardened cement paste [11, 23, 24], and the XRD results show that a new phase ($5Mg(OH)_2 \cdot MgSO_4 \cdot 7H_2O$) is formed in the hardened paste after adding citric acid [25–27]. In addition, the addition of citric acid can also prolong the setting time, and effectively improve the volume stability and water resistance of MOS [28].

At present, many researchers have carried out a series of research on the mechanical properties of MOS cement with different components, but the study on mechanical properties of MOS cement mixed with citric acid modifier under different molar ratio is still very rare. Under this background, the effects of $n(MgO) : n(MgSO_4) : n(H_2O)$ on the mechanical properties and durability of citric acid modified MOS cement were studied, and the pore distribution and phase change were analyzed by mercury intrusion method, XRD and TG. This study can provide important experimental basis for characterizing the performance of magnesium sulfate cement under different molar ratios.

2. Materials and experimental procedure

2.1. Materials

The light-burned magnesia powder is produced by Shijiazhuang magnesium Chemical Technology Co. Ltd., Hebei Province, China. The particle fineness is 120 mesh square hole sieve and its screen allowance is 2.1%, and the average particle size is 13.15 μm. The chemical composition and particle size distribution of light burned magnesia are shown in Table 1 and Fig. 1. Magnesium sulfate heptahydrate is an industrial grade magnesium sulfate produced by Xingtai Power Plant in Hebei Province, China. It is colorless, transparent, monoclinic and its purity is 99.1%. Its chemical composition is presented in Table 2. Citric acid ($C_6H_8O_7 \cdot H_2O$), produced by Beijing chemical plant, was used as additive to modify the mechanical properties of MOS cement. It is white crystal at room temperature with purity of 99.6%, and chemical composition are provided in Table 3.

Table 1. Chemical composition of light burned magnesia

Composition	MgO	SiO$_2$	CaO	Fe$_2$O$_3$	Al$_2$O$_3$
Content (wt %)	85.49	6.78	1.25	0.41	0.37

Table 2. Chemical composition of magnesium sulfate heptahydrate

Composition	MgSO$_4$	H$_2$O	MgCl$_2$	NaCl	Na$_2$SO$_4$
Content (wt%)	48.34	50.75	0.37	0.32	0.15
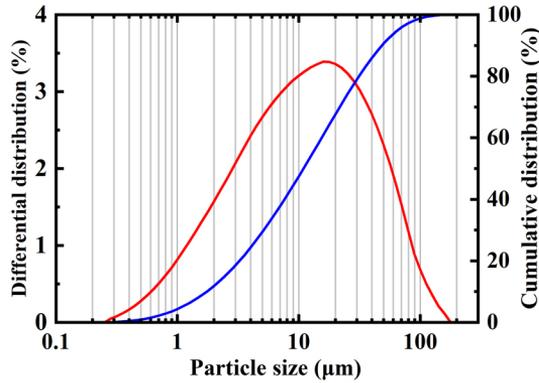
Fig. 1. Particle size distribution of light burned magnesia

Table 3. Chemical composition of citric acid

Composition	Insoluble matter	Cl	Ca	SO$_4$	PO$_4$	Fe
Content (wt %)	0.005	0.0005	0.004	0.005	0.001	0.0005

2.2. Preparation of MOS

The mixture proportions of the cement-based materials are displayed in Table 4. The mass ratio is calculated according to the content of active magnesium oxide (85%). According to the pre-test results of 7 d compressive strength, it is determined that the most reasonable citric acid content is 0.5%. A certain mass of MgSO$_4$·7H$_2$O crystal is dissolved in water to form a saturated magnesium sulfate solution, and then diluted with water to prepare magnesium sulfate solution with required concentration. According to the selected molar ratio of MgO : MgSO$_4$: H$_2$O, the amount of each raw material was calculated and weighed. Firstly, all the powder was mixed evenly, and then magnesium sulfate solution was incorporated into the powder. The mixing process was slow stirring (60 rpm) for 90 s, resting for 30 s and then rapid stirring (120 rpm) for 90 s.

2.3. Testing methods

2.3.1. Compressive and flexural strength

A YAW-300 microcomputer automatic compression and flexural strength machine was applied to test the 3 d, 7 d and 28 d mechanical strength of 40× 40× 160 mm specimen. The test method was carried out according to GB/T 17671-1999. The compressive strength and flexural strength of each specimen was measured, and the average value of flexural strength of three specimens and compressive strength of the six specimens were taken as the final result of the test.

Table 4. Mix proportions of citric acid modified MOS cement paste

No.	Mole ratio (mol)			Mass ratio (100g)		
	MgO	MgSO$_4$	H$_2$O	Light-burned magnesia	MgSO$_4$·7H$_2$O	H$_2$O
1	8	1	16	48.00	31.36	20.64
2	9	1	16	50.93	29.58	19.49
3	10	1	16	53.56	28.00	18.44
4	8	1	18	45.89	29.98	24.13
5	9	1	18	48.82	28.34	22.84
6	10	1	18	51.45	26.9	21.65
7	8	1	20	43.96	28.72	27.32
8	9	1	20	46.89	27.21	25.9
9	10	1	20	49.50	25.88	24.62

2.3.2. Water resistance

The softening coefficient was used to characterize the water resistance of MOS cement. Typically, the strength of MOS cement decreases with the extension of time due to the dissolution of water in the immersion environment. Therefore, the strength retention rate after immersion in water was defined as softening coefficient to characterize the water resistance of MOS cement. After standard curing for 28 days, the specimens were placed in water with temperature of 20° for 7 days. Then the moisture on the surface of specimens were wiped off and the compressive and flexural strengths after immersion were measured. The water softening coefficient of the specimen is as follows:

$$(2.1) \qquad R_f = \frac{R_{(w,7)}}{R_{(a,28)}}$$

where:

R_f – water softening coefficient of test piece after soaking in water for 7 days,
$R_{(w,7)}$ – strength of specimen before immersion in water, MPa,
$R_{(a,28)}$ – strength of specimen after immersion in water, MPa.

2.3.3. Volume shrinkage

The size of MOS cement specimen for measuring volume shrinkage is 10 mm × 10 mm × 60 mm. Firstly, the prepared MOS cement paste was poured into the mold and placed in curing box. The curing temperature was 25° and the relative humidity was 65%. The volume V_0 was accurately measured by drainage method, and then the volume V_n was measured again after curing to 28 days. The volume shrinkage of test sample is shown in Eq. (2.2):

$$(2.2) \qquad \varepsilon = \left(\frac{V_0 - V_n}{V_0} \right) \times 100\%$$

2.3.4. Pore structure

An AutoPoreIV9510 high performance automatic mercury injection instrument produced by Micromeritics instrument Ltd. in USA was used. The aperture measurement range of the instrument is 4 nm ÷ 120 μm. The cement paste specimens were cured to the predetermined age, crushed and took out a 1 cm × 1 cm × 1 cm cube small sample, and put the sample into anhydrous ethanol to stop its hydration. Before the test, the sample was put into a 50° vacuum drying oven to dry for 24 h and sealed with a sealed bag for testing.

2.3.5. XRD

After curing to the predetermined age, the cement paste specimens were crushed and then put into anhydrous ethanol to stop hydration. Before the test, the fragments were taken out and dried in a 50° vacuum drying oven for 24 h. The fragments were ground with a mortar, screened and refined with a 325 mesh sieve. 1 g pure sample powder was taken and sealed with a sealed bag. A Bruker D8 advance X-ray diffractometer (Cu Kα radiation, 30 mA, 40 kV) was used to characterize the samples.

2.3.6. TG-DTG

The Mettler Toledo TGA3 thermogravimetric analyzer was used to record the TG-DTG curves. Before the test, a part of the sample was taken, crushed and grinded into powder (< 100 μm) for the preparation of hydration stoppage, and then 50 mg of powder sample was taken into corundum crucible. The crucible was put into the instrument and the temperature was raised from 20° to 800°. the heating rate is 10°/min, and the gas flow rate of N_2 is 20 ml/min.

3. Results and discussion

3.1. Mechanical properties

The compressive strength of MOS cement specimens with different molar ratios after curing for 7 days is shown in Fig. 2(a). It can be found that with the extension of curing time, the compressive strength of MOS cement under the same mix proportion is significantly improved. Under the same curing time, the compressive strength is greatly affected by the molar ratio of MgO/MgSO$_4$ and H$_2$O/MgSO$_4$. When $n(H_2O)/n(MgSO_4)$ is fixed, the compressive strength of MOS cement increases with the increase of $n(MgO)/n(MgSO_4)$. When $n(MgO)/n(MgSO_4)$ is constant, the compressive strength decreases with the increase of $n(H_2O)/n(MgSO_4)$ molar ratio. For example, when $n(MgO):n(MgSO_4):n(H_2O) = 10:1:16$, the 28 d compressive strength of MOS cement is 65.4 MPa, while when $n(MgO):n(MgSO_4):n(H_2O)=8:1:20$, the compressive strength is as low as 50.7 MPa. However, when $n(H_2O)/n(MgSO_4) = 20$, the compressive strength with the molar ratio of 10:1:20 is lower than that of 9:1:20. The changing trend of flexural strength with molar ratio is similar to that of compressive strength (see Fig. 2(b)). With the increase of $n(MgO)/n(MgSO_4)$, the amount of MgO increases gradually, and the hydrolysis equilibrium of MgO in the system shifts to the right, which promotes the formation of phase providing strength and improves the mechanical strength of cement paste [29].
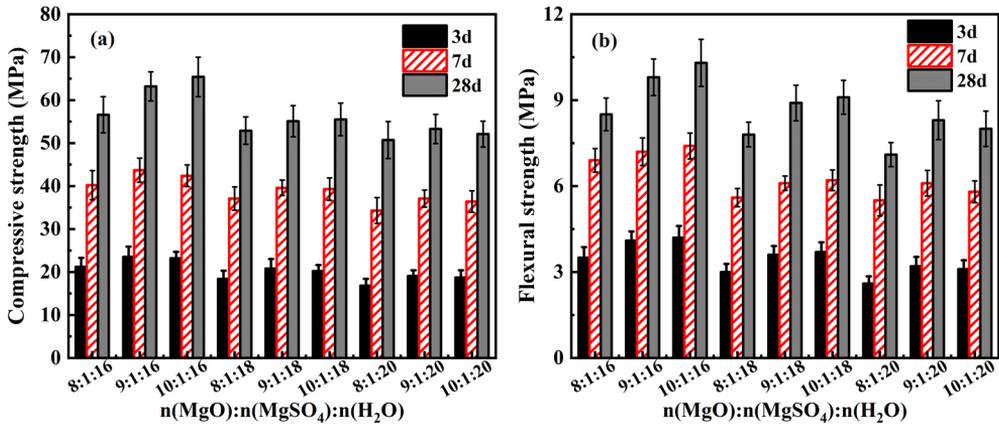
Fig. 2. Effect of MgO/MgSO$_4$/H$_2$O mole ratio on mechanical properties of MOS: (a) compressive strength vs. mole ratio, (b) flexural strength vs. mole ratio

3.2. Water resistance

Figure 3 shows the variation of softening coefficient of compressive strength and flexural strength of MOS cement after soaking in water for 7 days with different molar ratios. It can be seen from Fig. 3 that the softening coefficients of the hardened pastes with different molar ratios are all less than 1 after 7 days of immersion, indicating that the compressive strength has decreased to a certain extent. When $n(MgO) : n(MgSO_4)$ is constant, the softening coefficient of cement with $n(H_2O)/n(MgSO_4) = 18$ is the largest, showing the decrease range of compressive strength is the smallest. When $n(H_2O) : n(MgSO_4)$ remains the same, the softening coefficient decreases with the increase of $n(MgO)/n(MgSO_4)$. However, unlike the compressive strength
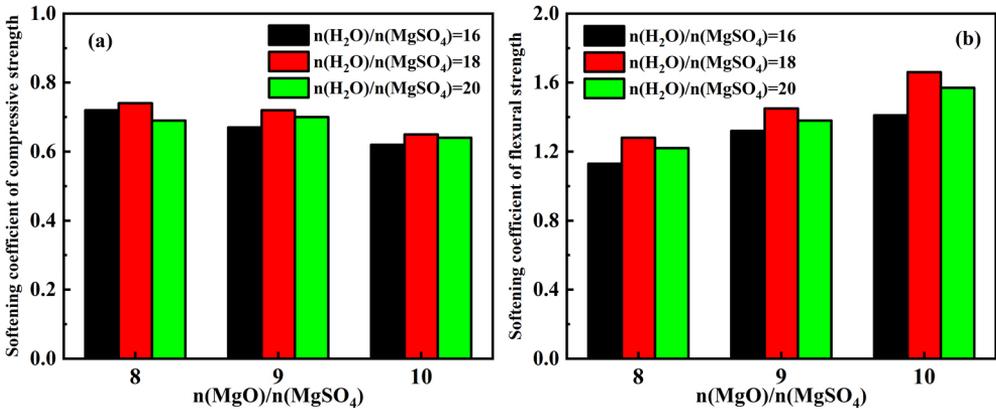
Fig. 3. Effect of molar ratio on softening coefficient of MOS cement: (a) Softening coefficient of compressive strength vs. molar ratio, (b) Softening coefficient of flexural strength vs. molar ratio

after immersion, the softening coefficient of flexural strength presents a different trend. The softening coefficients of pastes with all molar ratios are greater than 1, indicating that the flexural strength of pastes increases after 7 days of immersion. When $n(H_2O)/n(MgSO_4)$ remain unchanged, the softening coefficient increases with $n(MgO)/n(MgSO_4)$. After soaking in water, the hydration products ($MgCO_3$, 318 phase, etc.) outside the specimen gradually dissolve, resulting in the decrease of flexural strength. However, the unhydrated MgO particles in the specimen react with water immersed in specimen, which produces internal pressure in the structure, and then increases the flexural strength of hardened paste [28]. When the strength increase effect caused by internal hydration is greater than that caused by the dissolution of external hydration products, the flexural strength of MOS cement increases after immersion.

3.3. Volume shrinkage

Figure 4 presents the change of volume shrinkage rate with the mole ratio of MOS cement. As is shown in Fig. 4, the volume shrinkage decreases with $n(MgO) : n(MgSO_4)$, but increases with $n(H_2O)/n(MgSO_4)$. With the increase of MgO content, the hydration reaction rate of the system increases continuously and more strength phases are formed in the fixed space. The contact stress is formed inside the cement paste due to the hydration process, which improves the pore structure of the cement paste. When $n(MgO)$ is small or $n(H_2O)$ is large, the MOS cement paste is relatively thin at fresh stage. During the cement hardening process, the excess water will diffuse to the surface of the sample in the form of water vapor, which will form a large number of channels and make the internal of the cement become loose and increase the volume shrinkage rate. Choosing larger $n(MgO) : n(MgSO_4)$ and smaller $n(H_2O) : n(MgSO_4)$ can effectively reduce the volume shrinkage of MOS cement.
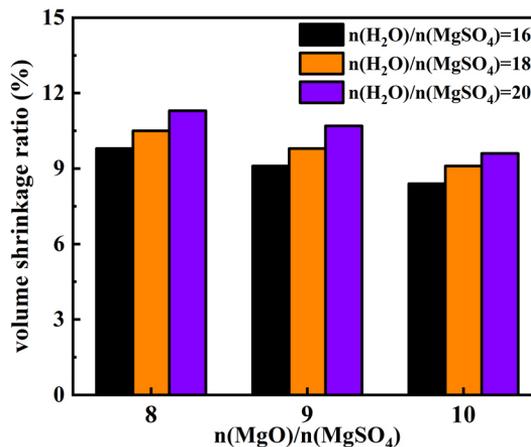
Fig. 4. Effect of molar ratio on volume shrinkage of MOS cement

3.4. Pore structure

Similar to PC, the strength and durability of MOS cement are closely related to its microstructure. Some researches show that the high porosity is the main reason for the low strength of MOS cement [30, 31]. The main pore structure parameters of MOS cement paste with different molar ratios are shown in Table 5. The increase of $n(MgO) : n(MgSO_4)$ decreases the porosity and other Aperture parameters of cement paste, on the contrary, the increase of $n(H_2O) : n(MgSO_4)$ increases the parameters.

Table 5. Pore structure parameters of MOS cement under different mole ratio

No.	MgO/ MgSO$_4$/ H$_2$O ratio	Porosity (%)	Total pore area (m$^2 \cdot$g^{-1})	Average pore diameter (nm)	Median pore diameter (nm)
1	8:1:16	13.47	11.89	11.44	15.75
2	10:1:16	10.84	8.56	10.86	12.91
3	8:1:20	15.76	14.03	13.89	17.56
4	10:1:20	13.08	11.75	10.97	13.25

In cement-based materials, the pores are usually divided into four categories: large pore (> 1000 nm), fine pore (100 ~ 1000 nm), transition pore (10 ~ 100 nm) and gel pore (< 10 nm) according to pore size [32–34]. The pore size distribution of magnesium oxysulfate cement under each molar ratio is shown in Fig. 5. The proportion of pores with 10 ~ 100 nm is the largest among the four different pore size range. By comparing the pore size distribution with the molar ratio of 8:1:16 and 10:1:16, it can be found that with the increase of the $n(MgO)$, the proportion of pores with pore size range less than 10 nm and 10–100 nm increases. When $n(H_2O)/n(MgSO_4) = 20$, the proportion of pores (< 100 nm) also increases with the increase of $n(MgO)$ ratio. Meanwhile, when the molar ratio of $n(MgO)/n(MgSO_4)$ is constant, the proportion of small holes < 100 nm decreases with the increase of H$_2$O molar ratio.
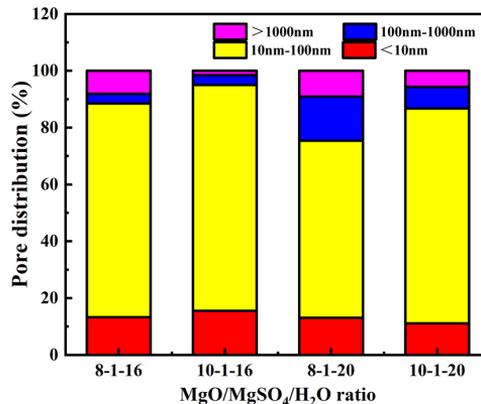
Fig. 5. Pore distribution of MOS cement with different molar ratio

In addition to counting the percentage of pores in each interval according to the size of diameter, the pore size distribution of the sample can also be characterized by the differential curve of mercury injection experiment. Figure 6 shows the curves of differential distribution of sample pore size, in which the peak value of the differential curve is the most probable aperture, i.e., the probability of pores appearing is the highest under this pore size. It can be seen from Fig. 6 that the most probable pore sizes of the four kinds of molar ratios of MOS cement are in the range of $10 \sim 100$ nm. The most probable pore size of paste with $n(MgO)$: $n(MgSO_4)$: $n(H_2O)$ = 8:1:20 is the largest (16 nm). The variation of the most probable pore size with the molar ratio is the same as that of the average diameter and the median diameter. When $n(H_2O)/n(MgSO_4)$ is larger or $n(MgO)/n(MgSO_4)$ is smaller, the most probable pore size of magnesium oxysulfate cement is larger. When the pore diameter is less than 10 nm, the amount of mercury in cement paste with the molar ratio of 10:1:16 is larger and there are many pores with small sizes. The cement paste with a molar ratio of 8:1:16 showed a sudden increase in mercury content near 260 nm, indicating that compared to other magnesium oxysulfate cement mixtures, there are still more large pores in the sample.
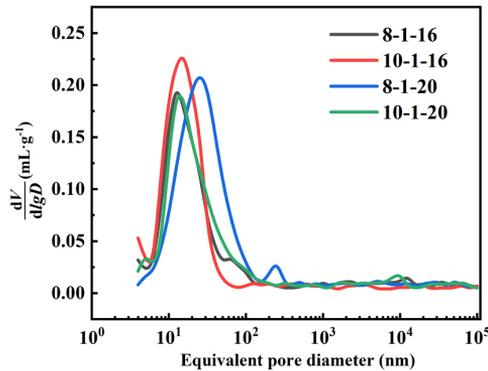
Fig. 6. Differential distribution of MOS cement at 28 d age

3.5. X-ray diffraction analysis

The phase composition of MOS cement after setting and hardening is uncertain due to the difficulty of complete chemical reaction in MgO–MgSO$_4$–H$_2$O ternary system. According to the previous researches, $3Mg(OH)_2 \cdot MgSO_4 \cdot 8H_2O$ (318 phase) in MOS cement can be stable at room temperature without adding any chemical additives, and 513 phase can be stably formed when the temperature is above 40°. However, a new peak appeared in the XRD spectrum after adding citric acid, which were confirmed as $5Mg(OH)_2 \cdot MgSO_4 \cdot 7H_2O$ magnesium oxysulfate phase (517 phase). 517 phase is the main product of magnesium oxysulfate cement system when its high hydration degree is high. It is a kind of short and coarse acicular crystal with good crystallinity, which can effectively improve the mechanical properties of magnesium sulfate cement [31, 35].

The XRD patterns of magnesium oxysulfate cement samples with different molar ratios are shown Fig. 7. It can be found from Fig. 7 that the main crystal phases in the citric acid modified MOS cement paste with different molar ratios are 517 phase, Mg(OH)$_2$, unreacted MgO,

undissolved $MgCO_3$ in light-burned magnesia and a small amount of SiO_2 from light-burned magnesia, but no 318 phase, which was in accordance with the results of Dinnebier et al. [36]. With the increase of $n(MgO)/n(MgSO_4)$, the peak strength of 517 phase increases, while that of $Mg(OH)_2$ is relatively weak. When $n(H_2O)/n(MgSO_4)$ increases, the intensity of 517 phase decreases. In the structure of hardened MOS cement paste, the formation of 517 phase can significantly improve the mechanical properties and later strength development of cement paste. The increase of $n(MgO)/n(MgSO_4)$ makes the content of 517 phase increase. On the contrary, the increase of $n(H_2O)/n(MgSO_4)$ inhibits the formation of 517 phase.

The XRD patterns of MOS cement incorporating citric acid with different molar ratio before and after immersed in water are shown in Fig. 8. For MOS cement with a molar ratio of
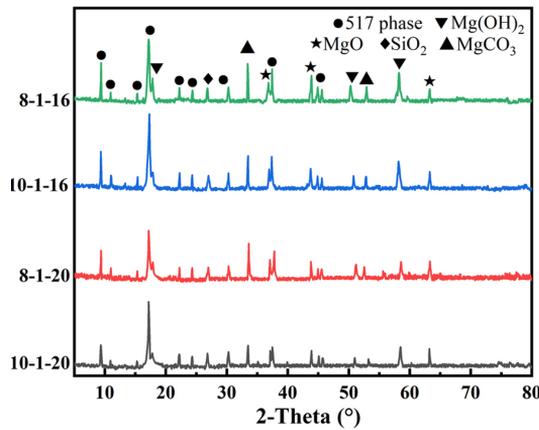
Fig. 7. XRD patterns of MOS paste with different $n(MgO) : n(MgSO_4) : n(H_2O)$ molar ratio at curing time of 28 days
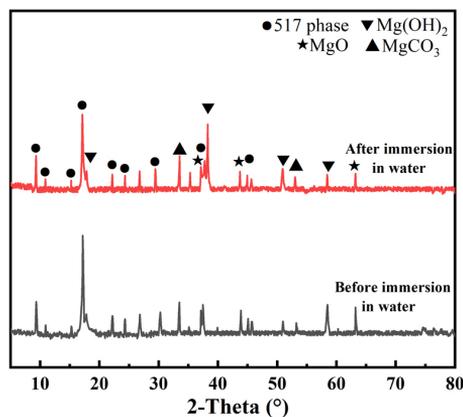
Fig. 8. XRD patterns of MOS paste before and after immersion in water for 7 days $(n(MgO) : n(MgSO_4) : n(H_2O) = 10:1:20))$

10:1:16 before immersion in water, the peak of 517 phase is stronger than that of $Mg(OH)_2$. After immersion in water for 7 days, the peaks of 517 phase and MgO decreased, while the peak of $Mg(OH)_2$ increased. The above results show that the 517 phase in the cement paste gradually decomposes under the reaction with water after immersing 7 days, resulting in the decrease of the compressive strength. However, the hydration reaction between MgO and external water promoted the further formation of $Mg(OH)_2$, which is more densely filled in the pores of cement paste. Although the strength of $Mg(OH)_2$ itself is not relatively high, the flexural strength increases after immersion due to its cementation in hardened MOS paste.

3.6. TG-DTG

Previous research [37] suggested that with the increase of temperature, magnesium oxysulfate cement containing 517 phase would undergo three main reaction processes, as shown in Eqs. (3.1)–(3.3):

$$(3.1) \quad 5Mg(OH)_2 \cdot MgSO_4 \cdot 7H_2O(s) \xrightarrow{80°\sim250°} 5Mg(OH)_2 \cdot MgSO_4(s) + 7H_2O$$

$$(3.2) \quad 5Mg(OH)_2 \cdot MgSO_4(s) \xrightarrow{300°\sim450°} 5Mg(OH)_2(s) + MgSO_4(s)$$

$$\xrightarrow{300°\sim450°} 5MgO(s) + 5H_2O + MgSO_4(s)$$

$$(3.3) \quad MgCO_3(s) \xrightarrow{500°\sim600°} MgO(s) + CO_2$$
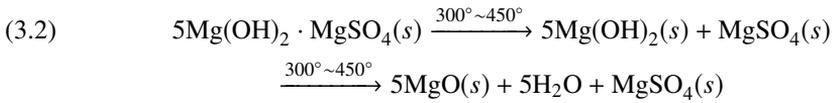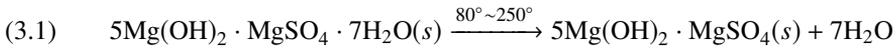
Figure 9 shows the thermogravimetric analysis results of magnesium oxysulfate cement specimens after curing for 28 days. It can be seen from Fig. 9 that the temperature range of weight loss reaction of paste with different molar ratio is basically consistent. Firstly, the mass of the sample began to decrease between 80° and 250°. At this time, the TG curve decreased significantly and the DTG curve showed the first large decline peak. This process was mainly due to the dehydration reaction of 517 phase to obtain anhydrous basic magnesium sulfate phase ($5Mg(OH)_2 \cdot MgSO_4$). According to the TG curve, the mass of the four groups of samples decreased by 1.48 mg, 1.39 mg, 1.67 mg and 1.51 mg at 250°, respectively. Then the mass proportion of 517 phase in MOS cement was calculated according to the molar mass of 517 phase and H_2O (shown in Table 6). It can be seen from the parameter results in the table that the content of 517 phase in magnesium oxysulfate cement paste with the molar ratio of 10:1:16 is the highest, while the content of 517 phase with the molar ratio of 8:1:20 is relatively the lowest. When the $n(MgO)/n(MgSO_4)$ is larger or the $n(H_2O)/n(MgSO_4)$ is smaller, the content percentage of 517 phase increases. The second weight loss occurred between 300° and 450°, during which $5Mg(OH)_2 \cdot MgSO_4$ was further decomposed into MgO, $MgSO_4$ and H_2O. In this stage, the mass of magnesium oxysulfate cement with four molar ratios decreased by 16.2%, 16.49%, 17.285% and 18.12% respectively. The third stage is the decarbonation of $MgCO_3$. During this period, the weight of the four groups of cement paste decreased by 3.89%, 3.69%, 4.40% and 4.26%, respectively.
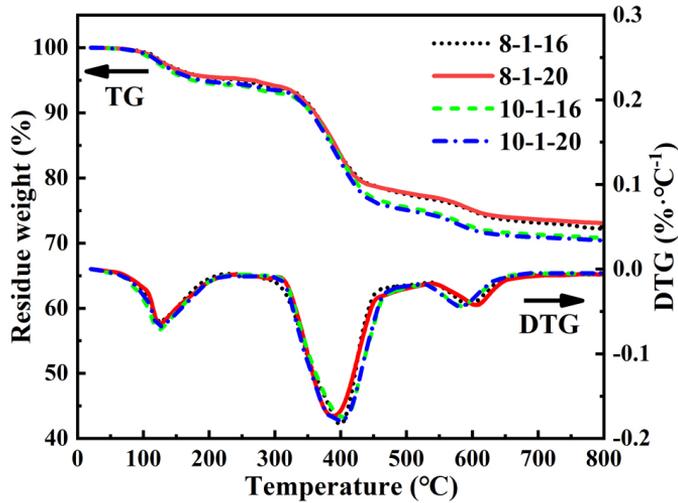
Fig. 9. Thermal analysis diagram of MOS cement pastes modified by citric acid at 28 days

Table 6. Variation of mass and other parameters of MOS cement in the first weight loss stage

No.	$n(\text{MgO}):$ $n(\text{MgSO}_4):$ $n(\text{H}_2\text{O})$	Sample mass	Weight loss	Weight loss percentage (%)	Mass of 517 phases	Relative content of 517 phase (%)
1	8:1:16	29.8mg	1.48	4.96	6.30	21.1
2	8:1:20	29.4mg	1.39	4.73	5.91	20.1
3	10:1:16	28.7mg	1.67	5.82	7.10	24.7
4	10:1:20	27.1mg	1.51	5.57	6.42	23.6

3.7. SEM

Figure 10 shows the SEM morphology of MOS pastes at different molar ratios after 28 days of curing. It can be found that hardened magnesium oxysulfate cement mainly consists of hexagonal flakes of magnesium oxide and some other hydration products with interlocking attachments. As the molar ratio of MgO : MgSO$_4$ increases, the content of layered magnesium oxide also increases. The microstructure formed by the interlaced hydration products of samples with a molar ratio of 8:1:20 is the densest. Meanwhile, Fig. 11 shows the microstructural differences of MOS paste before and after immersion in water for 7 days. It can be clearly observed that the density of the sample morphology decreases after immersion in water.
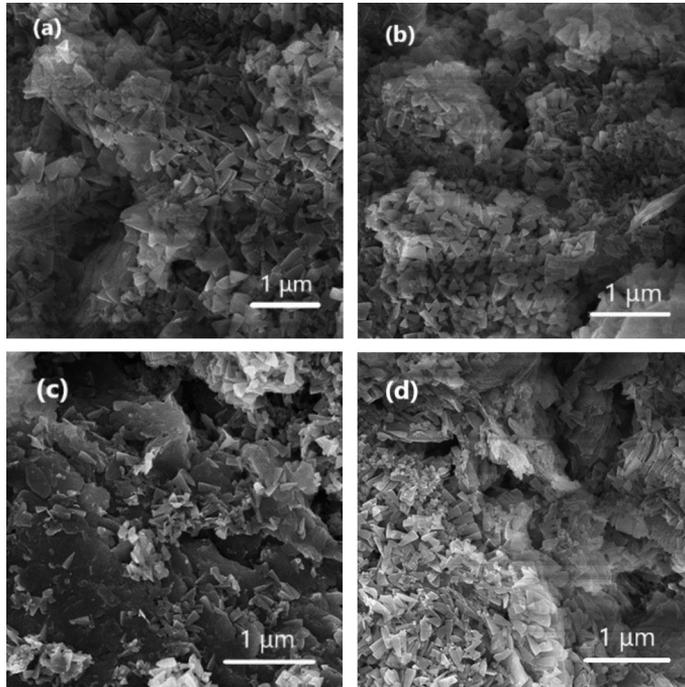
Fig. 10. Micromorphology of MOS paste cured for 28 d under different molar ratios of MgO : MgSO$_4$: H$_2$O showing: (a) 8-1-16 (b) 10-1-16 (c) 8-1-20 (d) 10-1-20
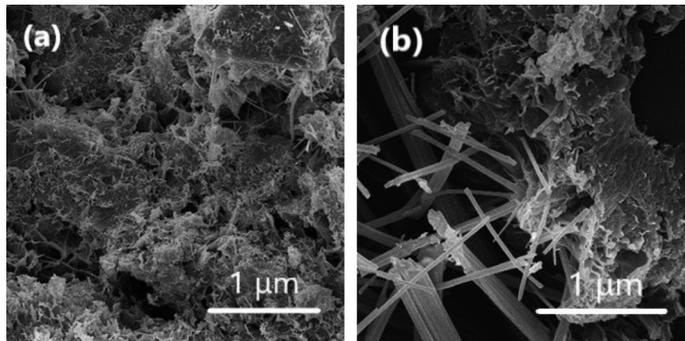
Fig. 11. Micromorphology of MOS paste with the molar ratio of 8:1:20 before (a) and after (b) immersion in water for 7 days

4. Conclusions

1. The higher the n(MgO)/n(MgSO$_4$) or n(MgSO$_4$)/n(H$_2$O), the greater the compressive strength and flexural strength of MOS cement paste. After immersion in water for 7 days, the compressive strength of cement paste decreases, while the flexural strength increases.

With the increase of $n(MgO)/n(MgSO_4)$, the softening coefficient of compressive strength decreases, while that of flexural strength increases. Small mole number of MgO or large mole number of H_2O correspond to high volume shrinkage rate of MgO cement paste.

2. The smaller the molar number of MgO or the larger the mole number of H_2O, the higher the pore structure parameters of cement paste. The most probable pore size of cement paste with $n(MgO) : n(MgSO_4) : n(H_2O) = 8:1:20$ is 16 nm. When $n(H_2O)/n(MgSO_4)$ is larger or $n(MgO)/n(MgSO_4)$ is smaller, the most probable pore size of MOS cement is larger.

3. With the increase of $n(MgO)/n(MgSO_4)$, the peak intensity of 517 phase in XRD patterns is high, while that of $Mg(OH)_2$ is relatively weak. When $n(H_2O)/n(MgSO_4)$ increases, the intensity of 517 phase decreases.

4. With the increase of temperature, magnesium oxysulfate cement containing 517 phase will undergo three weight loss processes. When the sample temperature rises to $250°$, the mass loss rate of MOS cement paste with the molar ratio of 10:1:16 is the highest, indicating that the content of 517 phase in the cement paste is the highest, while the content of 517 phase with the molar ratio of 8:1:20 is relatively low. The densest microstructure is formed by the interconnected hydration products of samples with a molar ratio of 8:1:20.

Acknowledgements

References

[1] I. Mehdipour, K. Aditya, and K.H. Khayat, "Rheology, hydration, and strength evolution of interground limestone cement containing PCE dispersant and high volume supplementary cementitious materials", *Materials and Design*, vol. 127, pp. 54–66, 2017, doi: 10.1016/j.matdes.2017.04.061.

[2] H. Manzano, J.S. Dolado, and A. Ayuela, "Elastic properties of the main species present in Portland cement pastes", *Acta Materialia*, vol. 57, no. 5, pp. 1666–1674, 2009, doi: 10.1016/j.actamat.2008.12.007.

[3] K. Celik, C. Meral, A.P. Gursel, P.K. Mehta, A. Horvath, and P.J. Monteiro, "Mechanical properties, durability, and life-cycle assessment of self-consolidating concrete mixtures made with blended portland cements containing fly ash and limestone powder", *Cement and Concrete Composites*, vol. 56, pp. 59–72, 2015, doi: 10.1016/j.cemconcomp.2014.11.003.

[4] Y. Peng, and C. Unluer, "Analyzing the mechanical performance of fly ash-based geopolymer concrete with different machine learning techniques", *Construction and Building Materials*, vol. 316, art. no. 125785, 2022, doi: 10.1016/j.conbuildmat.2021.125785.

[5] Y. Nie, J. Shi, Z. He, B. Zhang, Y. Peng, and J. Lu, "Evaluation of high-volume fly ash (HVFA) concrete modified by metakaolin: Technical, economic and environmental analysis", *Powder Technology*, vol. 397, art. no. 117121, 2022, doi: 10.1016/j.powtec.2022.117121.

[6] C. Chen, C. Wu, H. Zhang, Y. Chen, J. Niu, F. Chen, and H. Yu, "Effect of superplasticisers and their mechanisms of action on magnesium oxysulfate cement properties", *Advances in Cement Research*, vol. 32, no. 5, pp. 225–233, 2020, doi: 10.1680/jadcr.18.00001.

[7] X. Luo, W. Fan, C. Li, Y. Wang, H. Yang, X. Liu, and S. Yang, "Effect of hydroxyacetic acid on the water resistance of magnesium oxychloride cement", *Construction and Building Materials*, vol. 246, art. no. 118428, 2020, doi: 10.1016/j.conbuildmat.2020.118428.

[8] M.A. Haque, B. Chen, Y. Liu, S.F.A. Shah, and M.R. Ahmad, "Improvement of physico-mechanical and microstructural properties of magnesium phosphate cement composites comprising with Phosphogypsum", *Journal of Cleaner Production*, vol. 261, art. no. 121268, 2020, doi: 10.1016/j.jclepro.2020.121268.

[9] T. Runčevski, C. Wu, H. Yu, B. Yang, and R.E. Dinnebier, "Structural characterization of a new magnesium oxysulfate hydrate cement phase and its surface reactions with atmospheric carbon dioxide", *Journal of the American Ceramic Society*, vol. 96, no. 11, pp. 3609–3616, 2013, doi: 10.1111/jace.12556.

[10] Z.G. Li, Z.S. Ji, L.L. Jiang, and S.W. Yu, "Effect of additives on the properties of magnesium oxysulfate cement", *Journal of Intelligent and Fuzzy Systems*, vol. 33, no. 5, pp. 3021–3025, 2017, doi: 10.3233/JIFS-169353.

[11] C. Wu, H. Yu, J. Dong, and L. Zheng, "Effects of Material Ration, Fly Ash, and Citric Acid on Magnesium Oxysulfate Cement", *ACI Materials Journal*, vol. 111, no. 3, art. no. 291, 2014, doi: 10.14359/51686723.

[12] M. Ba, T. Xue, Z. He, H. Wang, and J. Liu, "Carbonation of magnesium oxysulfate cement and its influence on mechanical performance", *Construction and Building Materials*, vol. 223, pp. 1030-1037, 2019, doi: 10.1016/j.conbuildmat.2019.07.341.

[13] C. Wu, H. Yu, H. Zhang, J. Dong, J. Wen, and Y. Tan, "Effects of phosphoric acid and phosphates on magnesium oxysulfate cement", *Materials and Structures*, vol. 48, no. 4, pp. 907-917, 2015, doi: 10.1617/s11527-013-0202-6.

[14] Y. Peng and C. Unluer, "Development of alternative cementitious binders for 3D printing applications: A critical review of progress, advantages and challenges", *Composites Part B: Engineering*, vol. 252, art. no. 110492, 2023, doi: 10.1016/j.compositesb.2022.110492.

[15] C. Wu, C. Chen, H. Zhang, Y. Tan, and H. Yu, "Preparation of magnesium oxysulfate cement using magnesium-rich byproducts from the production of lithium carbonate from salt lakes", *Construction and Building Materials*, no. 172, pp. 597–607, 2018, doi: 10.1016/j.conbuildmat.2018.04.005.

[16] Y. Peng and C. Unluer, "Interpretable machine learning-based analysis of hydration and carbonation of carbonated reactive magnesia cement mixes", *Journal of Cleaner Production*, vol. 434, art. no. 140054, 2024, doi: 10.1016/j.jclepro.2023.140054.

[17] W. Chengyou, Z. Huifang, and Y. Hongfa, "Preparation and properties of modified magnesium oxysulfate cement derived from waste sulfuric acid", *Advances in Cement Research*, vol. 28, no. 3, pp. 178–188, 2016, doi: 10.1680/jadcr.15.00011.

[18] V. Barbieri, M.L. Gualtieri, T. Manfredini, and C. Siligardi, "Hydration kinetics and microstructural development of a magnesium oxysulfate cement modified by macromolecules", *Construction and Building Materials*, vol. 248, art. no. 118624, 2020, doi: 10.1016/j.conbuildmat.2020.118624.

[19] L. Xiang, F. Liu, J. Li, and Y. Jin, "Hydrothermal formation and characterization of magnesium oxysulfate whiskers", *Materials Chemistry and Physics*, vol. 87, no. 2–3, pp. 424–429, 2004, doi: 10.1016/j.matchemphys.2004.06.021.

[20] T. Demediuk and W.F. Cole, "A study of magnesium oxysulphates", *Australian Journal of Chemistry* vol. 10, no. 3, pp. 287–294, 1957, doi: 10.1071/CH9570287.

[21] L. Urwongse and C.A. Sorrell, "Phase relations in magnesium oxysulfate cements", *Journal of the American Ceramic Society*, vol. 63, no. 9-10, pp. 523–526, 1980, doi: 10.1111/j.1151-2916.1980.tb10757.x.

[22] J. Zhou and C. Wu, "Effects of nano-silica and silica fume on properties of magnesium oxysulfate cement", *Journal of the Ceramic Society of Japan*, vol. 128, no. 3, pp. 164–173, 2020, doi: 10.2109/jcersj2.19192.

[23] Q. Li, L. Zhang, X. Gao, and J. Zhang, "Effect of pulverized fuel ash, ground granulated blast-furnace slag and CO2 curing on performance of magnesium oxysulfate cement", *Construction and Building Materials*, vol. 230, art. no. 116990, 2020, doi: 10.1016/j.conbuildmat.2019.116990.

[24] J. Wen, H. Yu, Y. Li, C. Wu, and J. Dong, "Effects of citric acid on hydration process and mechanical properties of thermal decomposed magnesium oxychloride cement", *Journal of Wuhan University of Technology-Materials Science Edition*, vol. 29, no. 1, pp. 114–118, 2014, doi: 10.1007/s11595-014-0877-8.

[25] N. Zhang, H. Yu, N. Wang, W. Gong, Y. Tan, and C. Wu, "Effects of low-and high-calcium fly ash on magnesium oxysulfate cement", *Construction and Building Materials*, vol. 215, pp. 162–170, 2019, doi: 10.1016/j.conbuildmat.2019.04.185.

[26] H. Zhu, H. Yu, H. Ma, and S. Yang, "Uniaxial compressive stress-strain curves of magnesium oxysulfate cement concrete", *Construction and Building Materials*, vol. 232, art. no. 117244, 2020, doi: 10.1016/j.conbuildmat.2019.117244.

[27] Y. Tan, H. Yu, W. Bi, N. Wang, and N. Zhang, "Hydration Behavior of Magnesium Oxysulfate Cement with Fly Ash via Electrochemical Impedance Spectroscopy", *Journal of Materials in Civil Engineering*, vol. 31, no. 10, art. no. 04019237, 2019, doi: 10.1061/(ASCE)MT.1943-5533.0002827.

[28] N. Wang, H. Yu, W. Bi, Y. Tan, N. Zhang, C. Wu, H. Ma and S. Hua, "Effects of sodium citrate and citric acid on the properties of magnesium oxysulfate cement", *Construction and Building Materials*, vol. 169, pp. 697–704, 2018, doi: 10.1016/j.conbuildmat.2018.02.208.

[29] T. Guo, H. Wang, H. Yang, X. Cai, Q. Ma, and S. Yang, "The mechanical properties of magnesium oxysulfate cement enhanced with 517 phase magnesium oxysulfate whiskers", *Construction and Building Materials*, vol. 150, pp. 844–850, 2017, doi: 10.1016/j.conbuildmat.2017.06.024.

[30] C. Wu, W. Chen, H. Zhang, H. Yu, W. Zhang, N. Jiang, and L. Liu, "The hydration mechanism and performance of modified magnesium oxysulfate cement by tartaric acid", *Construction and Building Materials*, vol. 144, pp. 516–524, 2017, doi: 10.1016/j.conbuildmat.2017.03.222.

[31] J.J. Beaudoin and V.S. Ramachandran, "Strength development in magnesium oxysulfate cement", *Cement and Concrete Research*, vol. 8, no. 1, pp. 103–112, 1978, doi: 10.1016/0008-8846(78)90063-7.

[32] K. Liu, X. Cheng, C. Zhang, X. Gao, J. Zhuang, and X. Guo, "Evolution of pore structure of oil well cement slurry in suspension–solid transition stage", *Construction and Building Materials*, vol. 214, pp. 382–398, 2019, doi: 10.1016/j.conbuildmat.2019.04.075.

[33] W. Li, Y. Xie, K. Ma, G. Long, H. Zhao, and Y. Peng, "Multiscale mechanical evolution of the interface between self-compacting concrete and steam-cured concrete", *Journal of Building Engineering*, vol. 73, art. no. 106793, 2023, doi: 10.1016/j.jobe.2023.106793.

[34] W. Li, Y. Xie, K. Ma, G. Long, N. Li, W. Jiang, and Y. Peng, "Microstructure characteristics and evolution of the bonding interface between SCC and steam-cured concrete", *Construction and Building Materials*, vol. 400, art. no. 132837, 2023, doi: 10.1016/j.conbuildmat.2023.132837.

[35] T. Yue, S.Y. Gao, L.X. Zhu, S.P. Xia, and K.B. Yu, "Crystal growth and crystal structure of magnesium oxysulfate $2MgSO_4 \cdot Mg(OH)_2 \cdot 2H_2O$", *Journal of Molecular Structure*, vol. 616, no. 1-3, pp. 247–252, 2002, doi: 10.1016/S0022-2860(02)00347-2.

[36] R.E. Dinnebier, M. Pannach, and D. Freyer, "$3Mg(OH)_2 \cdot MgSO_4 \cdot 8H_2O$: A Metastable Phase in the System $Mg(OH)_2$-$MgSO_4$–H_2O", *Zeitschrift für Anorganische und Allgemeine Chemie*, vol. 639, no. 10, pp. 1827–1833, 2013, doi: 10.1002/zaac.201300128.

[37] B. Bissonnette, P. Pierre, and M. Pigeon, "Influence of key parameters on drying shrinkage of cementitious materials", *Cement and Concrete Research*, vol. 29, no. 10, pp. 1655–1662, 1999, doi: 10.1016/S0008-8846(99)00156-8.